IEEE Access
Multidisciplinary | Rapid Review | Open Access Journal

Received 5 October 2022, accepted 20 October 2022, date of publication 25 October 2022, date of current version 2 November 2022.

Digital Object Identifier 10.1109/ACCESS.2022.3216866

RESEARCH ARTICLE

Induced Overvoltage Caused by Indirect Lightning Strikes in Large Photovoltaic Power Plants and Effective Attenuation Techniques

AHMED I. OMAR[1], MOUSTAFA MOHSEN[1], MOUSA A. ABD-ALLAH[2], ZAKARIA M. SALEM ELBARBARY[3,4], AND ABDELRAHMAN SAID[2]

[1]Department of Electrical Power and Machines Engineering, The Higher Institute of Engineering at El-Shorouk City, El Shorouk Academy, Cairo 11837, Egypt
[2]Department of Electrical Engineering, Faculty of Engineering at Shoubra, Benha University, Cairo 11629, Egypt
[3]Electrical Engineering Department, College of Engineering, King Khalid University, Abha 61421, Saudi Arabia
[4]Electric Engineering Department, Faculty of Engineering, Kafrelsheikh University, Kafrelsheikh 33516, Egypt

Corresponding authors: Ahmed I. Omar (a.omar@sha.edu.eg) and Abdelrahman Said (abdelrahman.ghoniem@feng.bu.edu.eg)

This work was supported by the Deanship of Scientific Research, King Khalid University, under Grant RGP.1/ 223/43.

ABSTRACT Indirect Lightning Stroke (ILS) is considered an urgent issue on overall power systems due to its sudden dangerous occurrence. A grid-connected solar Photovoltaic (PV) power plant of 1MW was considered and analyzed using PSCAD/EMTDC software. The effect of grounding grid resistance (R_g) on the induced voltages caused by the indirect strokes was discussed. The Transient Grounding Potential Rise (TGPR) variation with R_g was presented and discussed. Four different models were proposed and installed for the system under study, which includes a combination of the Externally Gapped Line Arrester (EGLA) with the Non-Gapped Line Arrester (NGLA). The results show that when the R_g was reduced from 5 to 1 ohm, TGPR decreased by about 79.63%, whereas the peak value was reduced by about 91.3% nearby the striking position. Four models of EGLAs were proposed to reduce the induced transient overvoltage effectively. The four models showed a remarkable ability to reduce the backflow current (BFC) and, consequently, the induced overvoltage. The EGLA's type with the composite air gap reduced the TGPR by about 77.04 % and reduced the induced overvoltage nearby the striking position by about 51.3%.

INDEX TERMS ILS, EGLA, NGLA, backflow current (BFC), PV, grounding grid design (GGD), composite insulator, discharge voltage.

I. INTRODUCTION

Solar power generation will be indispensable for a sustainable source of power. Solar energy is a promising and beneficial source. Some precautions and protection requirements should be considered for the installed Photovoltaic (PV) power plant, whether standalone or grid-connected. Solar irradiation is widespread, and PV systems are built in open, outdoor spaces like solar farms or rooftops [1]. This makes surrounding electrical and electronic equipment vulnerable to lightning strikes. Air termination systems are put in place to deflect lightning strikes and guard the solar panels against direct harm. However, the air terminations allow high-value indirect lightning currents to enter the PV plant with high grounding resistivity due to high Transient Ground Potential Rise (TGPR) across the grounding system. These Backflow Currents (BFCs) pass through the Surge Protective Devices (SPDs), which are already installed in the design, causing high transient voltages through the system components [1], [2]. Over 50% of lightning-related electrical injuries yearly are caused by indirect lightning strikes, which are highly prevalent. On the other hand, just 4% of all electrical instances in a year include direct lightning strikes, as shown in Fig. 1 [3], [4].

The associate editor coordinating the review of this manuscript and approving it for publication was Giambattista Gruosso.

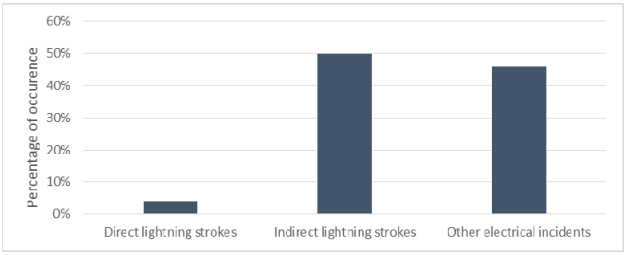

FIGURE 1. Percentage of direct and indirect lightning strokes to the world electrical incidents in a year.

Many studies have been carried out about this research approach for different systems, including the effect of BFCs on these systems and the analysis of the Grounding Grid Design (GGD) role. In [5], The simulation was run using a grid-connected solar PV plant located in Taif, Saudi Arabia, as an example, with a maximum generating output of roughly 1 MW, 22 arrays, 22 inverters, a power transformer, and an AC power grid make up the majority of the facility. The design of a modified PV grounding system is shown and assessed. Utilizing ATP/EMTP, the evaluation considers the backflow lightning overvoltage magnitudes at various places in the PV plant. In [6], this research investigates a thorough lightning surge analysis for offshore wind farms. Using ATP/EMTP, the overvoltages at the system's key nodes are determined using three lightning strike scenarios, and two surge arrester systems are suggested. The findings show that the surge caused by an onshore overhead line is the most dangerous circumstance. The benefits of the submarine cable are for lightning protection. Since all of the electrical equipment at an offshore power plant uses the same grounding, a backflow surge could enter the electrical system. In [7], this article proposes a computational model for lightning-induced voltage on PV systems using the Finite-Difference Time-Domain (FDTD) method and for the first time, the lightning-induced voltages for PV systems in challenging topography, such as flat land, lakes, and mountains, are investigated. A backflow current will enter the cable via SPD if lightning strikes the lightning rod in a region with high soil resistivity. However, one of the main factors in the PV system's decline is the overvoltage brought on by an indirect strike. Events occur more frequently than lightning strikes directly. In [8], this article's objective is to look at how grounding electrode performance when exposed to lightning strikes is affected by frequency-dependent soil models for a grounding system of the wind turbine. An effective numerical technique called the Method of Moments (MOM) is based on surface-wire integral equations. In comparison to the scenario when the parameters are presumed constant, numerical results show that the frequency dependency of the soil parameters causes a decrease in the potential rise of the grounding electrodes.

In [9], The influence of surge arresters, underbuilt grounded conductors, and shield wire on the direct and indirect lightning performance of medium voltage overhead lines are compared in the article. By taking into account, the impact of the structures next to the line that decreases the frequency of direct events and increases the frequency of indirect ones, the environmental shielding on the total lightning performance is also taken into account. The findings confirm that both strategies reduce the space between surge arresters or decrease grounding resistance, successfully enhancing lightning performance. In [10], The EMTP-RV program models a double-circuit 400 kV transmission line in a mountainous region. A thorough analysis is done to confirm the efficacy of using EGLA. The obtained results demonstrate that four EGLAs installed in the upper and middle phases with a downstream shield wire can provide an appropriate level of direct lightning protection for transmission lines. In [11], Four spans, each 400 meters long, have been used to represent the 63 kV transmission line on either side of the point of impact simulated by EMTP-ATP software. It is noticed that the overvoltage values for static and nonlinear resistors differ. This is because the electrical properties of the soil depend on ionization. As soil resistivity rises, the EGLA absorbed energy for lightning strikes to the phase conductor has decreased. As a result, the EGLAs experience reduced discharge current and have a longer anticipated life. For a brief summary for these past works and their limitations, Table 1 displays it concisely with showing the objective of this proposed work.

In this paper, a 1 MW grid-connected solar PV farm under indirect lightning impact made up of 42 PV arrays that each produce 24 kW at a temperature of 25° C and an irradiance of 1000 W/m^2. Each array has 96 PV modules, each of which has 60 multi-crystalline solar cells and produces 250 W of power at 29.8 V of voltage and 8.39 A of current. To connect to an 11-kW grid, this PV system uses 42 inverters, each rated at 20 kW, and a 1500 kVA three-phase step-up transformer. It is provided with a detailed analysis of the system under study to investigate the effect of the BFC through the system, which increases the transient peak voltages measured at different locations throughout the system by inducing discharge current and solutions are covered to reduce these transients appear through the system such as the effect of variation of the grounding resistance (R_g) on the passed BFC which affects directly on the TGPR measured across the R_g. As shown in the above literature, few studies included the usage of EGLA to reduce the ILS danger, and the installation of EGLAs was limited to Overhead transmission lines. So, four models are formed from a mix of an EGLA with Non-Gapped Line Arrester (NGLA), which improves the voltage profile after each critical component in the PV grid-connected power plant by decreasing the TGPR values by choosing the optimum model depending on the discharge voltage for each. As it is known about this study's methodology, the practical work is expensive and harmful to both grid components and people. Researchers are typically instructed to employ temporary software programs to study and apply their findings. In this paper, Power System Computer Aided Diagram/Electromagnetic Transient Direct

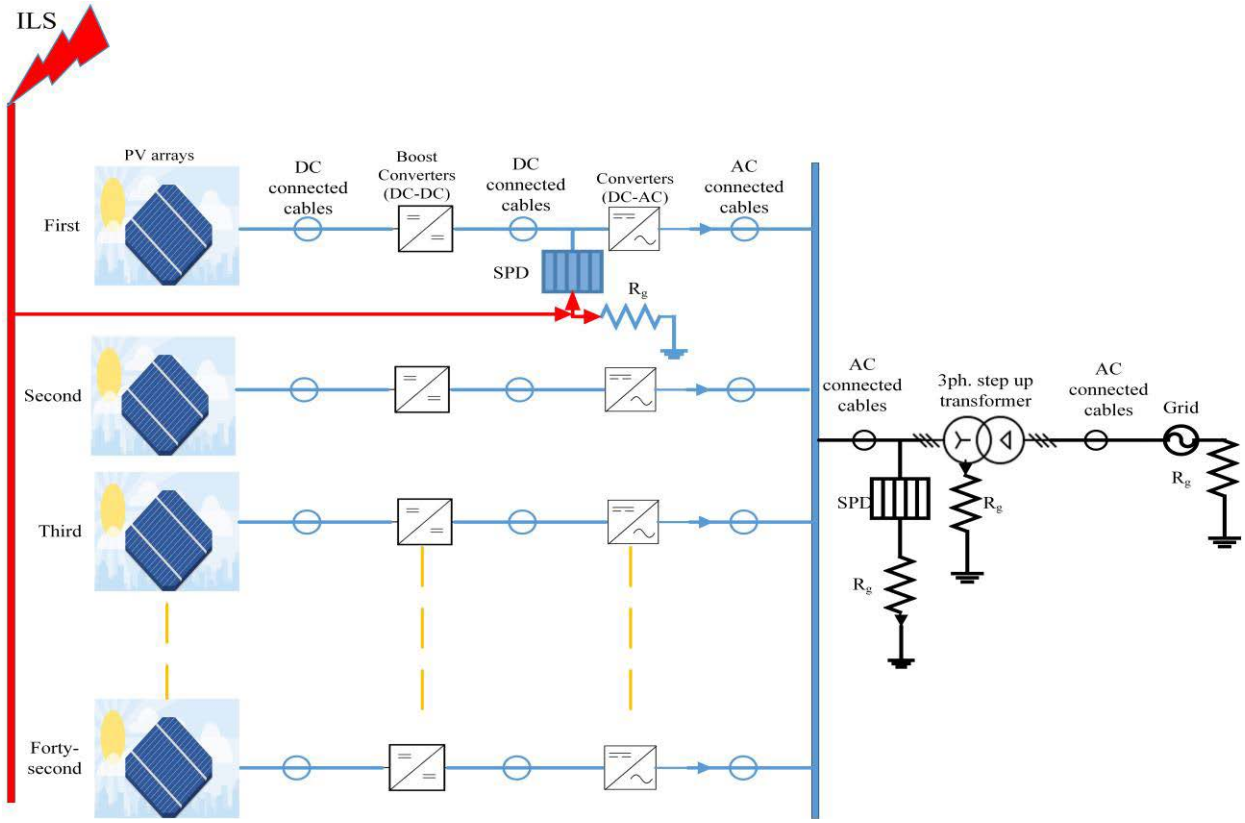

FIGURE 2. Line diagram for a PV grid-connected under study showing the ILS paths.

Current (PSCAD/EMTDC) was used for the simulation and analysis of the solar power plant under study with the aid of the Electrical Transient Analyzer Program (ETAP) software package for the simulation of the GGD at some specific R_g values.

The significant contributions of this study are as follows:

1. A crucial analysis of the effect of BFC at the most influential positions in the system considers the impact of the grounding resistance. Discuss the improved GGD at different grounding resistance values using ETAP software.
2. Choosing the optimal combination between EGLA and NGLA to effectively reduce the overvoltage transients and protect the sensitive points of the PV system from an indirect lightning stroke.

II. SOLAR PV PLANT OVERVIEW

A solar-tied grid farm was studied due to its prevalence and the most exposure to lightning strokes than other plants [12]. The single-line diagram of the PV farm under study is shown in Fig. 2. This is made up of 42 PV arrays and cables connecting them with the 11 kV grid, boost converters, inverters, and step-up transformers. Where the air termination that the ILS impacted is assembled with a down conductor, the ILS current finds more than one path through the system, either the SPDs or R_g. The general specifications of the PV system are listed in Tables 2 and 3 [13].

III. SOLAR PV PLANT MODELLING

Using PSCAD custom blocks for system design, the modeling of each component concerning the previously specified system was demonstrated in this part. The AC and DC cables are used to link these blocks operated at a 50 Hz frequency, considering the air termination simulated by a busbar presides the PV arrays with a grounding system for the solar PV plant.

A. PV FARM MODELLING WITHOUT EGLA

The PV system's components modeling parameters used in PSCAD are enumerated for each element in Table 4 and Table 5 with the aid of the parameters listed in Table 2 and Table 3 [13]. The SPD's (I-V) characteristic data are listed in Table 6. The IEEE model shown in Fig. 4 is used for SPD simulation in PSCAD, and its parameters are enumerated in Table 4.

B. EXTERNALLY GAPPED LINE ARRESTER MODELLING

SPD is considered one of the best mitigation techniques to reduce lightning stroke's effect, especially the direct one. For indirect lightning strokes, it doesn't work efficiently. As it becomes in a reverse position, it acts as a resistance for the resultant backflow current. So, EGLA is one of the

TABLE 1. Summary of the literature survey.

Ref.	Year	Cases			System under study	Comments
		BFC effect due to ILS	Grounding effect on the BFC	EGLA effect on the BFC		
[6]	2020	✓	✓	×	PV grid-connected power plant	By utilizing ATP/EMTP software, it was discussed a modified PV grounding system but the voltage profile still had some high values due to BFC
[7]	2022	✓	✓	×	offshore wind farm connected to an onshore overhead line through a submarine cable	This paper discussed the effect of grounding on this type of system with the installation of NGLA. Using ATP/EMTP proved that the discharge current reduced more with the reduction of grounding resistance.
[8]	2021	✓	×	×	PV grid-connected power plant	Using the (FDTD) method, a PV system was analyzed with a high soil resistivity. Using NGLA, the transient voltages were measured due to indirect stroke without discussing the effect of either grounding or EGLA.
[9]	2021	✓	✓	×	Wind turbine with its grounding system	Considering the MOM's numerical technique, the grounding electrode performance was analyzed for this system when it was exposed to lightning strikes. Numerical results show that the frequency dependency of the soil parameters causes a decrease in the potential rise of the grounding electrodes, but the system wasn't large and simple
[10]	2021	✓	✓	×	Medium voltage overhead transmission line system	The influence of surge arresters and underbuilt grounded conductors on the direct and indirect lightning performance. The findings confirm that both strategies reduce the space between surge arresters or decrease grounding resistance, successfully enhancing lightning performance.
[11]	2020	×	×	✓	a double-circuit 400 kV transmission line	The EMTP-RV program modeled this system in a mountainous region. A thorough analysis was done to confirm the efficacy of using EGLA. The obtained results demonstrated that four EGLAs installed in the upper and middle phases with a downstream shield wire could provide an appropriate level of direct lightning protection for transmission lines
[12]	2022	×	✓	✓	63 kV transmission line	EMTP-ATP was used to simulate this system by applying different lightning strokes. This is because the electrical properties of the soil depend on ionization. As a result, the EGLAs experience reduced discharge current and have a longer anticipated life.
Proposed	2022	✓	✓	✓	Large PV grid connected power plant	All cases are discussed for a large PV grid-connected power plant with particular analysis for the EGLA models that wasn't used before for PV system but used in [11] for overhead transmission line system.

best solutions for this type of lightning strokes. EGLA is composed of a gap distance and a non-linear metal-oxide resistor. Its MCOV value depends on the IEC 60099-8 standard, which must be higher than the system rating, about 1.1 of the maximum line-to-neutral voltage at its installation. When lightning strikes, the spark gap ignites, securely discharging the excess voltage through the ensuing arc. The EGLA application enhances the design of the power systems, lowers the cost of construction and maintenance, and dramatically improves the performance and operation of the power systems [14], [15].

The four models shown in Fig. 3 for EGLA with SPDs, sometimes called Non-Gapped Line Arrester (NGLA), are considered, and also the IEEE model is considered for NGLA modeling, shown in Fig. 4 [10]. The best EGLA model chosen depends on the most absorbent for the discharge voltage through it, which decreases the transient voltages that appear through the system under study due to the backflow current passing through the air termination settled for the PV arrays when the lightning strokes are applied. Through analysis of the transient response of discharge voltage, the performance of four types of EGLA (Types 1, 2, 3, and 4) are examined

TABLE 2. PV array system and boost converter specifications.

Components	Specifications	Value
PV arrays system	# of series modules	24
	No. of parallel module strings	4
	Ref. irradiance	1000 W/m^2
	Ref. cell temperature	25 °C
	# of series cells	60
	# of parallel cell strings	1
	Open circuit voltage (V_{oc}) per module	37.6 V
	Short circuit current (I_{sc}) per module	8.81 A
	Max. power (P_{max}) per module	250.192 W
	The voltage at max. power point (V_{MPP}) per module	30.4 V
	Current at max. power point (I_{MPP}) per module	8.23 A
	Temperature Coeff. of V_{oc} ($\%/deg.^oc$) per module	-0.31782
	Temperature Coeff. of I_{sc} ($\%/deg.^oc$) per module	0.05782
Boost converter	# of converters	42
	Max. power rating	0.024 MW
	Max. power point tracking (MPPT)short circuit current of PV array	0.03524 kA
	MPPT open circuit voltage of PV array	0.9024 kV
	MPPT tracked algorithm	Incremental conductance (InC)

TABLE 3. VSC, transformer, GRID, cable, and SPD specifications.

Components	Specifications	Value
VSC	Nominal AC power	20 kW
	Reactive power set-point	-0.1 MVAr
	DC voltage set point	720 V
	d-axis current upper bound	1 kA
	q-axis current upper bound	0.3 kA
Transformer	3-φ MVA	1.5 MVA
	Winding#1 type	Earth connected star
	Winding#2 type	Delta
	Winding#1 line voltage	433V
	Winding#2 line voltage	11kV
Grid	3- φ base MVA	1.5 MVA
	Base voltage	11 kV
	+ve sequence impedance; phase shift	0.25 Ω; 80°
Cable	Cable length	10 m
	System frequency	50 Hz
	Rated MVA	1.5 MVA
	Rated voltage	720 V_{dc}, 400 V_{ac} at inverter side, 11 kV_{ac} at transformer side
SPD	Voltage of arrester at DC side	0.8 kV
	A voltage of arrester at AC side	0.5 kV
	Arrester inputs Ch.'s	ASEA XAP-A

where the EGLA is represented by a spark gap whose on resistance is 0.01 ohms and the off resistance is 10^6 Ω. The arrowed part in each type, as shown in Fig. 3, is the NGLA one [4], [10].

The form of EGLA's Type 2 air gap is made up of a composite insulator and air, as shown in Fig. 5, with gap distance depending on the voltage range used in the system and also the sphere diameter used according to IEEE 516-2009 standard shown in Table 7 [16]. The air gap and composite insulator type are represented by the paralleled capacitors C_o and C_c, respectively, where the composite material used is the ceramic (Si_3N_4) material with relative permittivity (ε_r) equals 8.3 [10], [17].

The formulas used to calculate the equivalent capacitance (C_t) and voltage (V_c) across the composite gap are shown in (1) and (2), and the composite gap voltage is the function of the angular frequency (ω) and the EGLA's Type 2 parameters used are shown in Table 7.

$$C_t = C_c + C_o \tag{1}$$

$$|V_c| = \frac{1}{\omega C_t} \tag{2}$$

TABLE 4. Modelling parameters for the PV array and boost converter in PSCAD.

Components	Parameters	Values
PV array	Adequate area for each cell	0.01 m^2
	Series resistance for each cell (R_s)	0.34034 Ω
	Shunt resistance for each cell (R_{sh})	187.6477 Ω
	Diode ideality coefficient	0.95043
	Saturation current at the ref. conditions for each cell	$62.179*10^{-12}$ kA
	Short circuit current at the ref. conditions for each cell	0.03342 kA
	Temperature factor of photocurrent	0.0564
Boost converter (DC-DC)	K_p boost	2
	T_i boost	0.5
	D_{max} boost	0.21

TABLE 5. Modeling parameters for the voltage *source* converter and SPD in PSCAD.

Components	Parameters	Values
Voltage Source Converter (VSC) (DC–AC)	*Kp_dc*	0.5
	Ti_dc	0.2
	Kp_Q	0.3
	Ti_Q	0.02
	Kp_d	0.15
	Ti_d	0.08
	Kp_q	0.15
	Ti_q	0.08
SPD	R_o	54.19 Ω
	R_1	37.54 Ω
	L_o	0.421 µH
	L_1	2.217 µH
	C_s	1.08 nF

IV. RESULTS AND DISCUSSION

A. BEHAVIOR OF PV POWER PLANT UNDER NORMAL OPERATION

The forty-two arrays of the PV farm were rearranged into three networks for investigation, as depicted in Fig. 6. The first network consists of a single array with an inverter and boost converter and produces around 24 kW. The other two networks have about 488 kW with the exact PV array specifications but with a different number of parallel module strings. A boost converter and an inverter with customized specifications connect each network.

Due to its constrained simulation run points, PSCAD's lengthy EMTDC run time is reduced using this system reduction technique. The system was validated in [13], where the steady-state waveforms with time for the array voltage, current, and power at P1 in the PV farm shown in Fig. 6 and the output AC voltage and current following the VSC are noted. The steady-state values for the output AC voltage and current from the inverter and the output DC voltage, current, and power from the PV array are enumerated in Table 8.

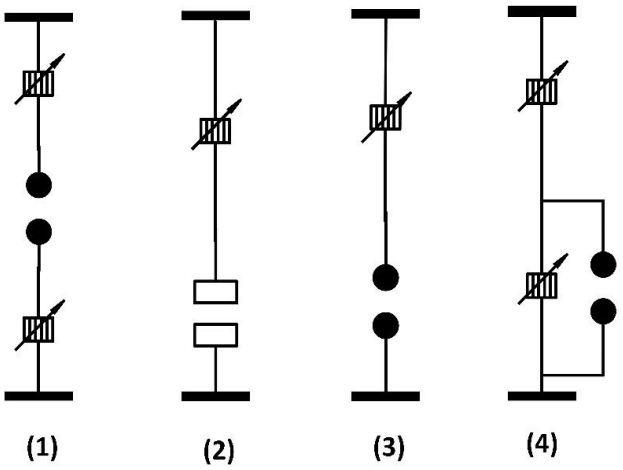

FIGURE 3. Different models for EGLA with NGLA.

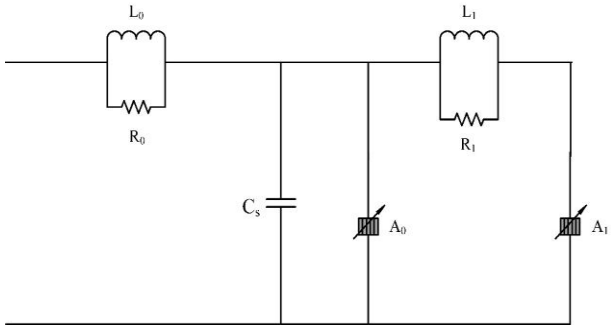

FIGURE 4. PSCAD's IEEE frequency-dependent SPD model.

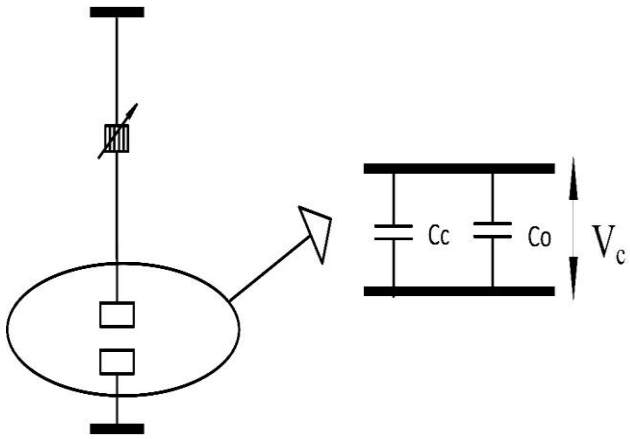

FIGURE 5. EGLA's Type 2 air gap equivalent model.

TABLE 6. I-V characteristic data of ASEA XAP-A for the used SPD.

Current A)	0.001	0.01	0.1	0.2	0.38	0.65	1.11	1.50	2.00	2.80
Voltage (V)	1.100	1.60	1.70	1.739	1.777	1.815	1.853	1.881	1.910	1.948

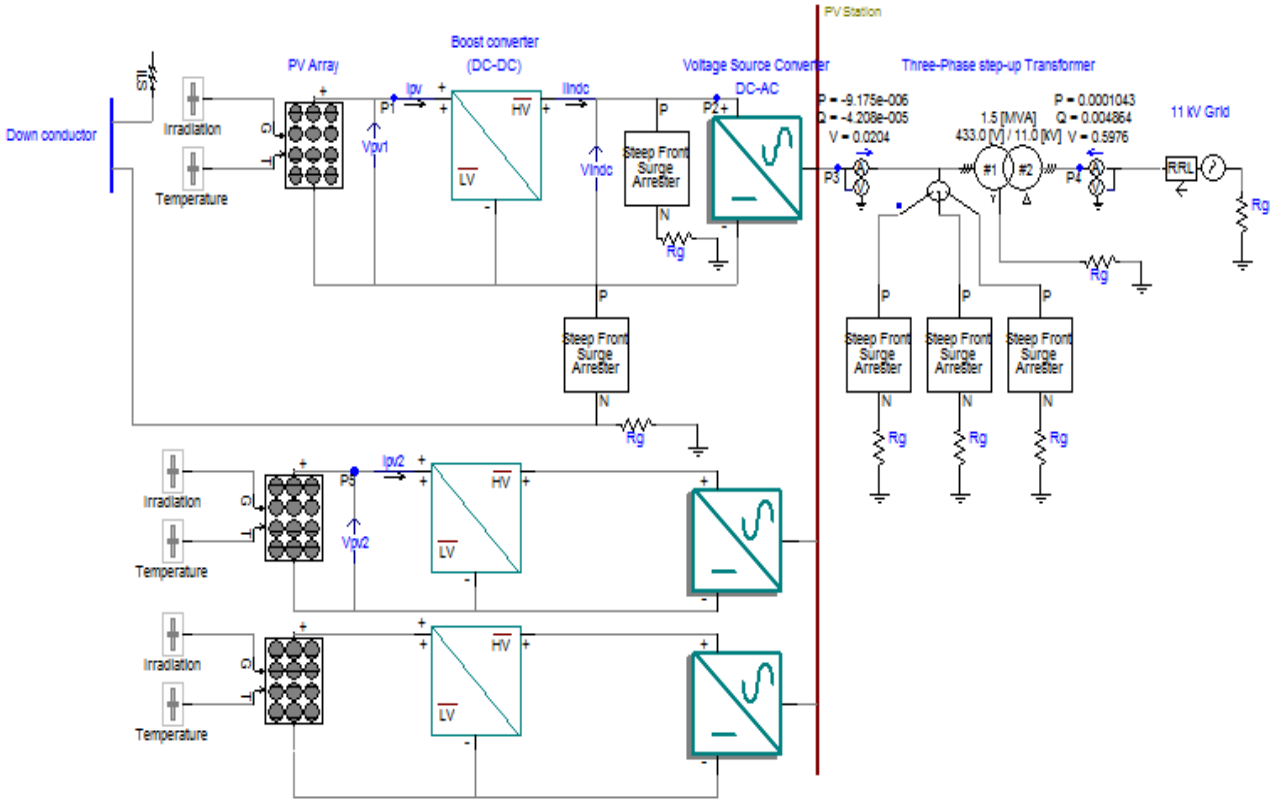

FIGURE 6. Solar PV system under the effect of ILS in PSCAD.

TABLE 7. EGLA's type 2 parameters' specifications.

EGLA's Type 2 parameters	Specifications
Gap distance	0.02 m
Gap diameter	0.2 m
The dielectric constant for ceramic material	8.3
Airgap simulated capacitance	55.6 pF
Ceramic material simulated capacitance	461 pF

TABLE 8. The first PV array and the inverter output parameters under normal operation for the system under study.

The output steady-state parameters for the system under study	Values
$V_{PV\ array1}$	715.2 V
$I_{PV\ array1}$	33.4 A
$P_{PV\ array1}$	0.024 kW
V_{VSC}	380 V
I_{VSC}	37.8 A

B. BEHAVIOR OF PV POWER PLANT UNDER INDIRECT LIGHTNING STROKES

There is common grounding between the DC and AC parts of the system through R_g. The effect of ILS is investigated by reconfiguring the PV system after the installation of SPD according to CLC 50539-12 standard and considering the impact of the grounding resistance as shown in Fig. 6. Its line diagram is shown in Fig. 2. Where the down conductor assembles the installed air termination. The ILS current flows through the down conductor when the lightning stroke applied at the down conductor is 200 kA 0.25/100 μs which finds more than one path through the SPDs and the R_g. So, transient voltages are induced at different positions overall in the system under study due to the BFC passing through the SPDs, which would negatively affect each component in the system. Therefore, improving the grounding resistance or the SPDs installed is necessary to reduce these high transient dangers voltages.

C. EFFECT OF GROUNDING GRID RESISTANCE ON THE TRANSIENT VOLTAGES INDUCED DUE TO ILS

System grounding grid design is one of the best and costless solutions offered by researchers to absorb most of the ILS current passed through the down conductor [5], [6]. The high soil resistivity of the grounding grid leads to less current leakage to the earth, and more BFC passes through the SPDs, resulting in the high transient voltage appearing through the system [18], [19]. IEC 60364 defines the standardized earthing systems schemes, which also ensures that R_g is less than 5 ohms for the excellent quality earthing system and, therefore, can be used for the PV plant.

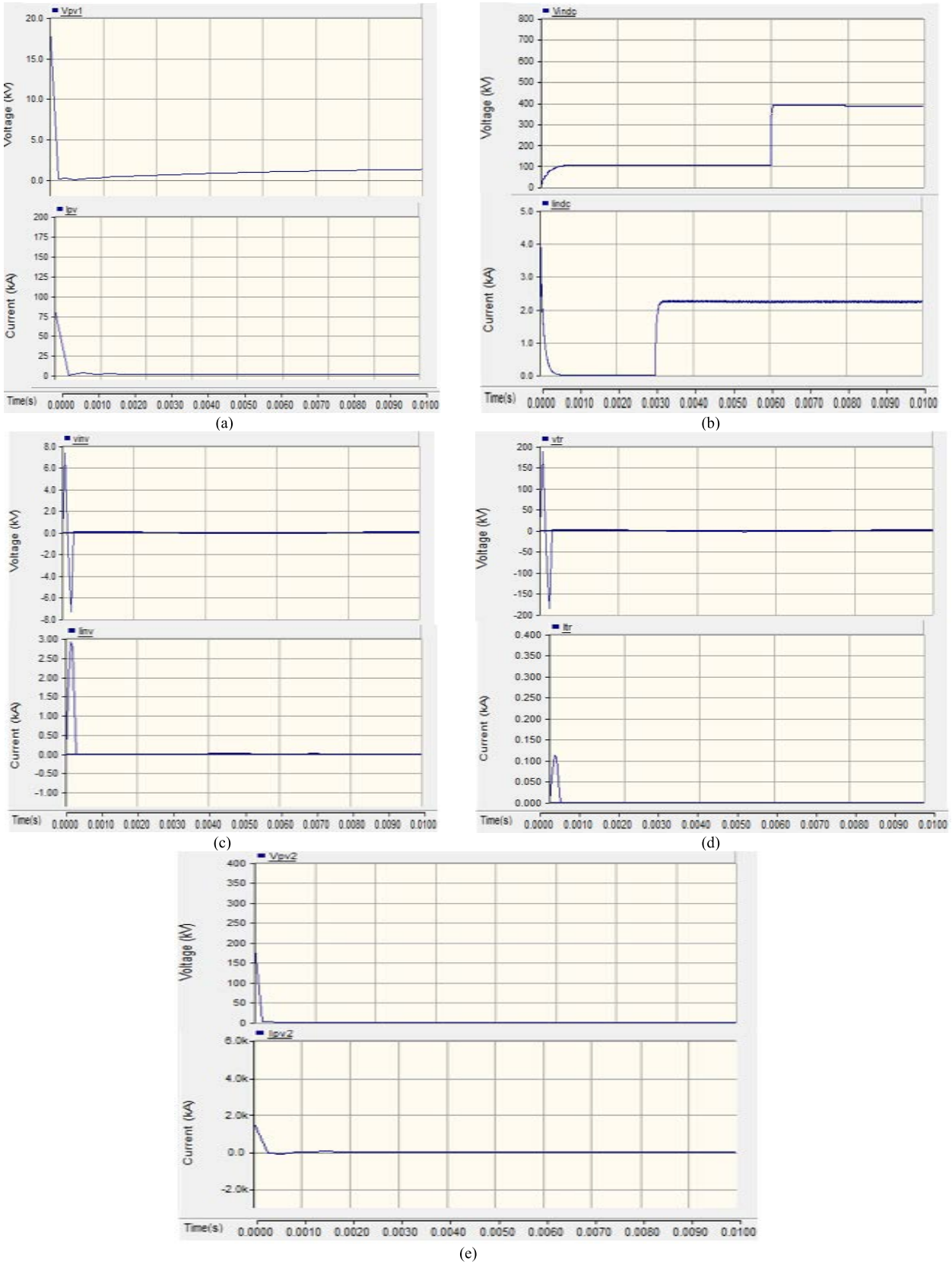

FIGURE 7. The grounding resistance at 5 Ω (a) Measured voltage and current waveforms at P1; (b) Measured voltage and current waveforms at P2; (c) Measured voltage and current waveforms at P3; (d) Measured voltage and current waveforms at P4; (e) Measured voltage and current waveforms at P5.

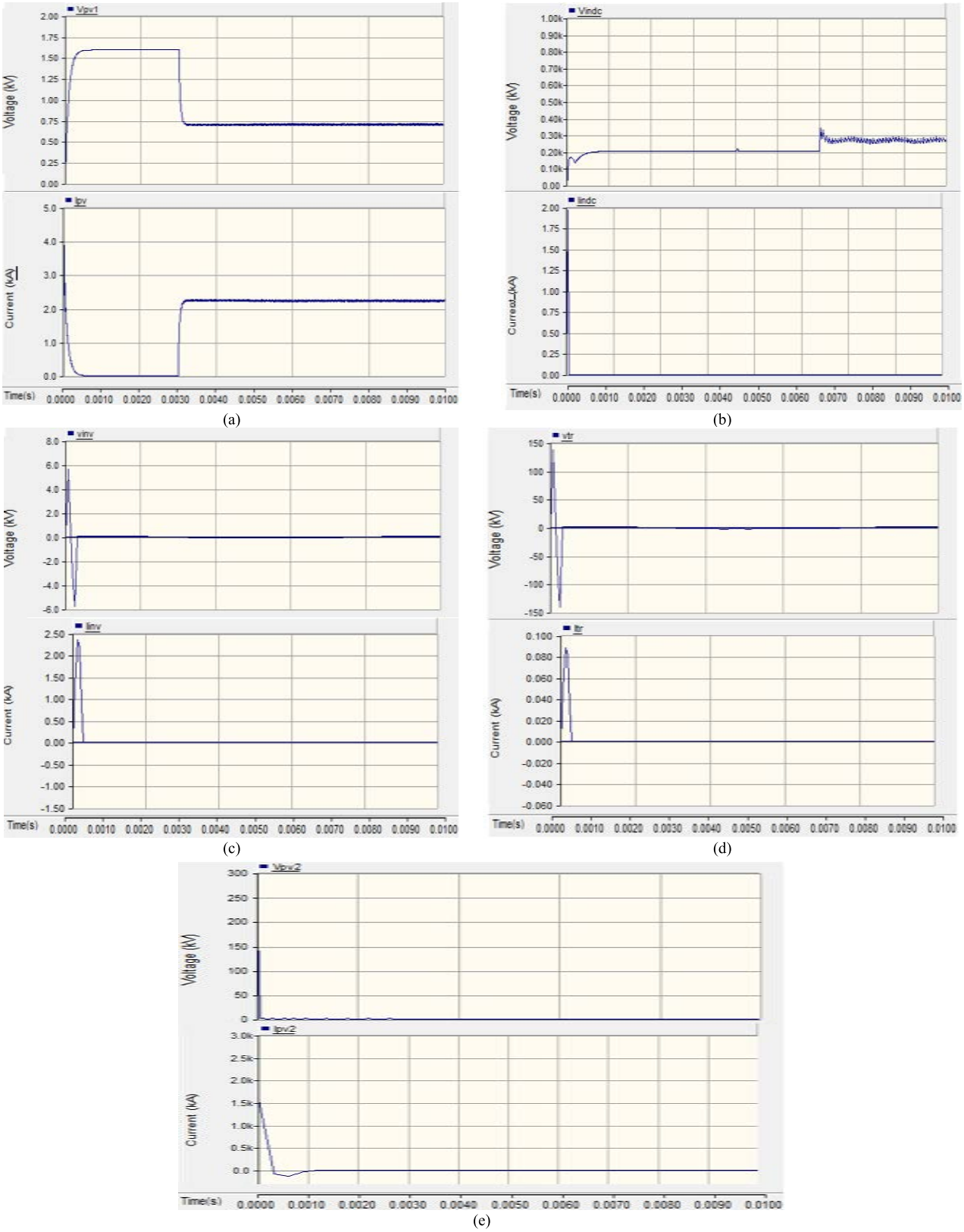

FIGURE 8. The grounding resistance at 1 Ω (a) Measured voltage and current waveforms at P1; (b) Measured voltage and current waveforms at P2; (c) Measured voltage and current waveforms at P3; (d) Measured voltage and current waveforms at P4; (e) Measured voltage and current waveforms at P5.

TABLE 9. Variation of the measured peak voltages with the grounding resistance.

Measured peak voltage (kV) / R_g (Ω)	V_g	$V_{P@P1}$	$V_{P@P2}$	$V_{P@P3}$	$V_{P@P4}$	$V_{P@p5}$
5	1.08 x 10^3	18.4	380.3	7.9	195.6	180.7
4	0.83 x 10^3	15.1	372.6	7.5	180.3	174.8
3	0.64 x 10^3	10.9	365.8	6.7	171.8	162.7
2	0.41x 10^3	5.8	349.6	6.2	160.2	149.2
1	0.22x 10^3	1.6	340.4	5.8	145.8	144.6

TABLE 10. TGPR measured in different study cases.

Mitigation technique	V_g (kV)	
	Value	Reduction (%)
Using NGLA and Rg = 1 Ω	221.3	0 %
Using Type 1 with Rg = 1 Ω	110.4	50.11%
Using Type 2 with Rg = 1 Ω	50.8	77.04%
Using Type 3 with Rg = 1 Ω	135.7	38.68%
Using Type 4 with Rg = 1 Ω	90.1	59.29%

So, for discussing the effect of variation of grounding grid resistance on the transient voltage induced in the system that already its grounding grid is designed, the grounding resistance will be changed from 5 to 1 ohm, and the lightning stroke applied at the down conductor is 200 kA 0.25/100 μs then the transient voltages at the positions indicated at Fig. 6 are recorded and listed at Table 9. Moreover, the TGPR is measured across the grounding resistance, which is the ground potential (V_g) which it is responsible for the grounding system current value at each case from 5 to 1 ohm for showing to what extent the ground leakage current is the danger for the design and listed in Table 9 and, the transient voltages waveforms recorded over the different indicated positions at Rg equals to 5 Ω and 1 Ω are shown in Fig. 7 and Fig. 8 respectively. As the grounding resistance decreases from 5 Ω to 1 Ω, the measured peak transient voltage also reduces by about 91.3% at P1, and this decrease appears at all different positions in the system. Moreover, the TGPR also decreases by approximately 79.63%, indicating that more current leaks as the resistance decreases and the measured peak voltages at different positions are areduceuced due to less BFC passing. Using the ETAP software, the GGD for each PV array chosen (Jinko Solar JKM250P-60 module) can be implemented, and its area is about 14.4 m×4 m (47.24 ft.×13.12 ft.). As shown in Fig. 9 (a), the GGD in Three Dimension (3D) form for the PV array at R_g equals 5 Ω, where the number of conductors in the X direction and Y direction is (3 × 6) conductors with using 14 rods. As shown in Fig. 9 (b), the GGD in 3D form the PV array at R_g equals 1 Ω, where the number of conductors in the X direction and Y direction is (3 × 11) conductors using 20 rods.

When the R_g equals 1 Ω, the voltage and current waveforms at P1, as shown in Fig. 8(a), reach Steady State (SS) waveforms but still with high values both for the voltage and current there and also for the other chosen positions. The voltage at P1 equals 1.6 kV, and the current equals 3.9 kA.

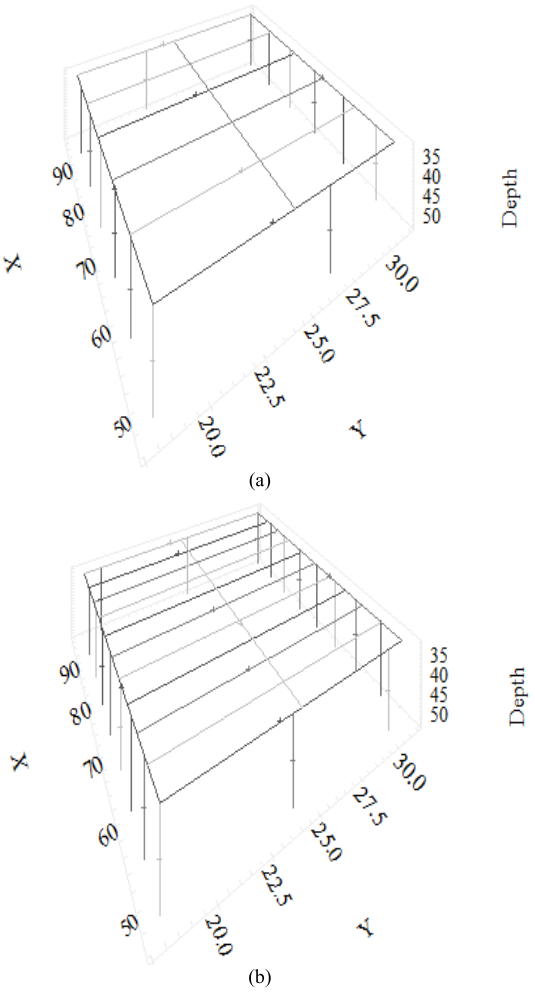

FIGURE 9. GGD in 3D form using ETAP at R_g equals (a) 5 Ω, (b) 1 Ω.

So, these values still are a danger for the system under study components, and it is necessary to mitigate this danger by other alleviation techniques, such as using the different models of EGLA shown in Fig. 3.

TABLE 11. Comparison between using each model of EGLA earlier mentioned with $R_g = 1\ \Omega$ and using NGLA with $R_g = 1\ \Omega$.

Measured peak voltage / Mitigation technique	$V_{P@p1}$		$V_{P@p2}$		$V_{P@p3}$		$V_{P@p4}$		$V_{P@p5}$	
	Value (kV)	%red*	Value (kV)	%red*	Value (kV)	%red*	Value (kV)	%red*	Value (kV)	%red*
Using NGLA	1.6	0 %	340.4	0 %	5.8	0 %	145.8	0 %	144.6	0 %
EGLA's Type 1	1.1	31.3%	98.2	71.2%	1.05	81.9%	16.1	89 %	108.4	25.03%
EGLA's Type 2	0.78	51.3%	57.6	83.1%	0.45	92.2%	15.8	89.2 %	33.2	77.04%
EGLA's Type 3	1.18	26.3%	105.8	68.9%	1.2	79.3%	18.3	87.5 %	112.4	22.27%
EGLA's Type 4	1.03	35.63	70	79.4%	0.8	86.2%	15.6	89.3%	100.4	30.57

%red.* = %reduction

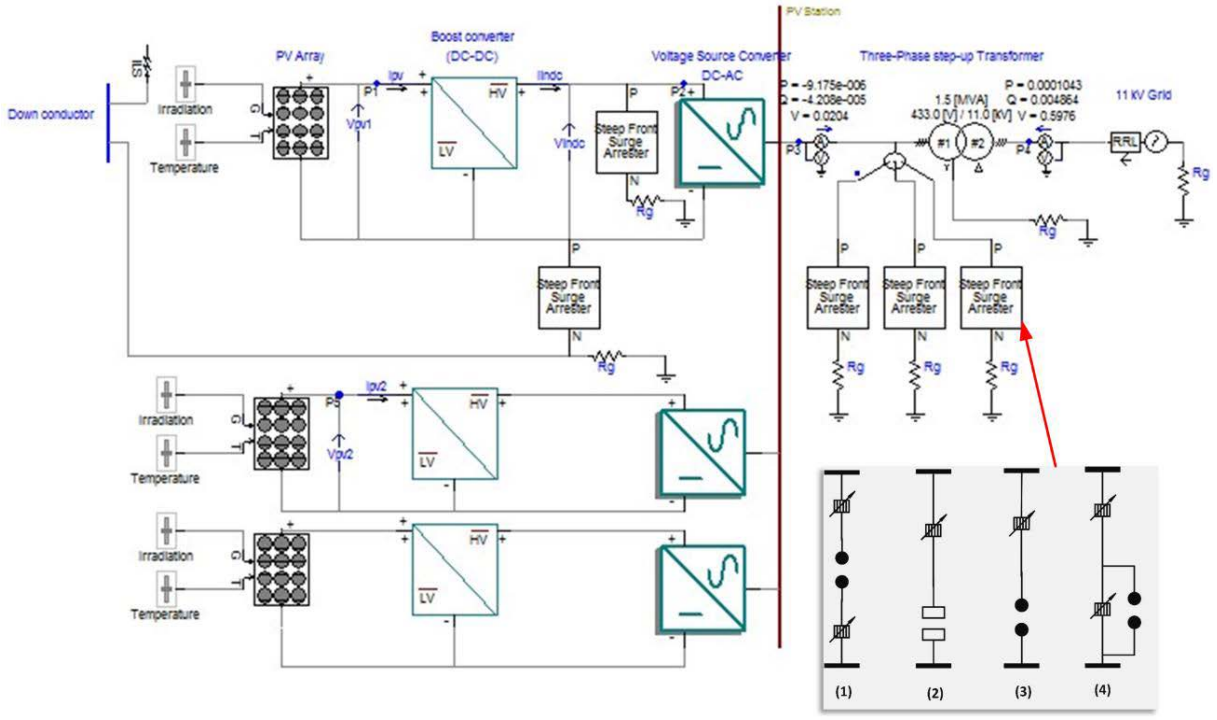

FIGURE 10. Solar PV system under the effect of ILS with the EGLAs' models proposed in PSCAD.

D. EFFECT OF USING EGLA ON THE TRANSIENT VOLTAGES INDUCED DUE TO ILS

Although the grounding resistance value was reduced to 1 Ω, the values of the induced transient voltages due to the flow of BFC through the system are still high, as shown in Fig. 8. Therefore, it is directed to resist the BFC through the SPD as demonstrated in Fig. 6, to decrease these transient voltages. Researchers used the EGLA technique to protect the

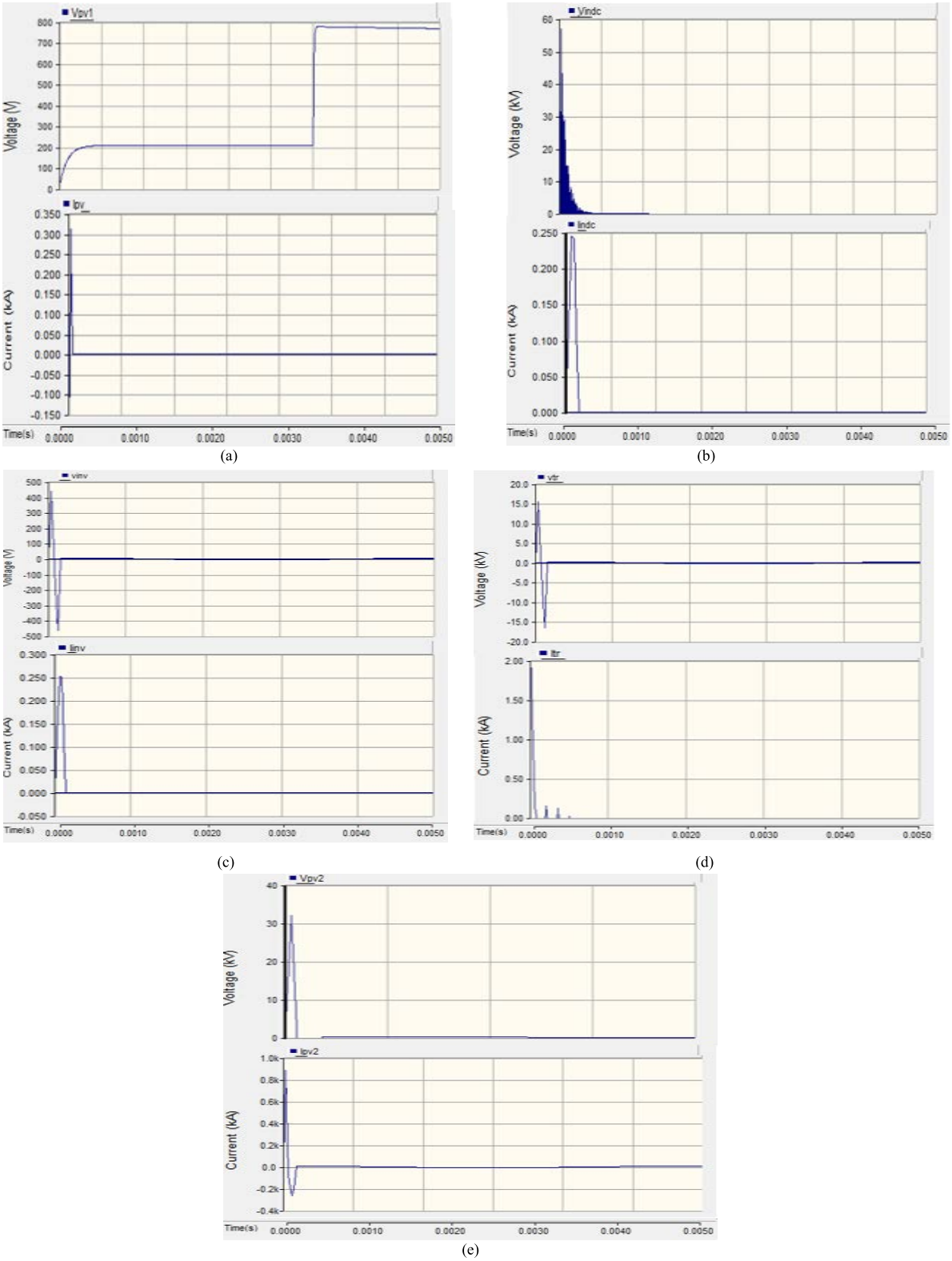

FIGURE 11. Type 2 of the EGLA's (a) Measured voltage and current waveforms at P1; (b) Measured voltage and current waveforms at P2; (c) Measured voltage and current waveforms at P3; (d) Measured voltage and current waveforms at P4; (e) Measured voltage and current waveforms at P5.

transmission line systems. In this study, four models composed of EGLA and NGLA were used instead of an SPD at PV farms,s, as shown in Fig. 10.

Where the EGLA is represented in PSCAD by a spark gap, its breakdown voltage or MCOV at the installation location is approximately 1.1 of the maximum line to

neutral voltage. The IEEE model shown in Figure 4 is used to model the NGLA. These models shown in Figure 3 are simulated in PSCAD separately by replacing the system's NGLA [19], [20].

After several varieties are considered, the best type of line arrester is selected for higher withstand voltage. The discharge voltage serves as the criterion for comparing the various EGLA kinds. Because of fixed composite insulators, Type 2 has an externally fixed gap and does not alter the air gap in stormy situations.

Type 2 has a higher discharge voltage than other variants. The various structures of the air-gap model are to account for this. This air gap can resist higher voltages than different types because it can withstand a high lightning strike current. As a result, it stops the arrester's active portion (NGLA), the arrowed part shown in Figure 3, from failing to function. In reality, after the same lightning strike, Type 2 dielectric breakdown happens after the breakdown of the other types.

According to Fig. 3, the air gap in this kind of EGLA is made up of a composite insulator and air combination. The air gap and composite insulator types are represented by the paralleled capacitors C_0 and C_c, respectively, as shown in its equivalent model in Fig. 5 [14], [21].

Table 10 shows the TGPR measured across the R_g for each case of mitigation techniques by using each type separately and the peak voltages measured at the proposed positions in the system shown in Fig. 10. These voltages are listed in Table 10 after replacing every kind by the NGLA type installed when the grounding resistance equals to 1 Ω, where these measured values are compared with those obtained when the grounding resistance equals 1 Ω. The NGLA type is installed before replacement.

As discussed in [10] for overhead transmission lines, the use of Type 2, which contains the composite gap, achieves a high mitigation percentage in comparison with the other types and, of course, is better than using only the NGLA type with keeping the grounding resistance lower and equals to 1 Ω as shown in Table 10 and Table 11 and also ensured at the waveforms shown in Fig. 11 compared with that shown in Fig. 8. Moreover, the reduction in the TGPR is high which show obviously how EGLA's Type 2 resist the flow of the BFC through it roughly. This elevated alleviation percentage is reached due to the composite material used in Type 2 provides preferable results in comparison with other types, and also, it is also characterized by less weight than the three types used. Type 3 offers fewer mitigation percentages at all chosen positions but less weight than Types 1 and 4.

V. CONCLUSION

The effect of grounding resistance, installation of NGLA, and the four proposed types of EGLA with the 1 Ω grounding resistance on the transient overvoltages were discussed. It was concluded that the ILS current finds a path to flow through the SPDs in the system in case of good grounding systems or not where a lightning stroke of 200 kA, 0.25/100 μs, was applied at the down conductor. The main conclusions are:

1- Improving the grounding grid reduces the BFC and the induced transient overvoltage. As the grounding resistance decreases from 5 Ω to 1 Ω, the measured peak transient overvoltage was reduced by about 91.3% at P1, and the TGPR decreased by approximately 79.63%. Despite this significant reduction in induced overvoltage, the voltage values are still high.
2- At a higher grounding resistance, it is recommended to replace the NGLA with one of the suggested models for EGLA to reduce the BFC effectively.
3- EGLA's Type 2 is the preferable model, which effectively reduces the induced overvoltage than the other types at the indicated positions in the system. For P1, the transient overvoltage reduces by about 51.3% when the EGLA's Type 2 was installed beside the R_g equals 1 Ω.

REFERENCES

[1] N. I. Ahmad, M. Z. A. Ab-Kadir, M. Izadi, N. Azis, M. A. M. Radzi, N. H. Zaini, and M. S. M. Nasir, "Lightning protection on photovoltaic systems: A review on current and recommended practices," *Renew. Sustain. Energy Rev.*, vol. 82, pp. 1611–1619, Feb. 2018, doi: 10.1016/j.rser.2017.07.008.

[2] K. Damianaki, C. Christodoulou, C.-C. Kokalis, A. Kyritsis, E. Ellinas, V. Vita, and I. Gonos, "Lightning protection of photovoltaic systems: Computation of the developed potentials," *Appl. Sci.*, vol. 11, no. 1, p. 337, Dec. 2020, doi: 10.3390/app11010337.

[3] A. A. Kusuma, P. A. A. Pramana, B. B. S. D. A. Harsono, and B. S. Munir, "Effect of indirect lightning strike to 66kV transmission line in Java-Bali system," in *Proc. MATEC Web Conf.*, vol. 197, Sep. 2018, p. 11001, doi: 10.1051/matecconf/201819711001.

[4] F. Giraudet, "Various benefts for line surge arrester application and advantages of externally gapped line arresters," in *Proc. Int. Conf. High Voltage Eng. Technol. (ICHVET)*, Feb. 2019, pp. 1–6, doi: 10.1109/ICHVET.2019.8724171.

[5] N. A. Sabiha, M. Alsharef, M. K. Metwaly, E. E. Elattar, I. B. M. Taha, and A. M. Abd-Elhady, "Sustaining electrification service from photovoltaic power plants during backflow lightning overvoltages," *Electr. Power Syst. Res.*, vol. 186, Sep. 2020, Art. no. 106386, doi: 10.1016/j.epsr.2020.106386.

[6] Q. Sun, L. Yang, Z. Zheng, J. Han, Y. Wang, and L. Yao, "A comprehensive lightning surge analysis in offshore wind farm," *Electr. Power Syst. Res.*, vol. 211, Oct. 2022, Art. no. 108259, doi: 10.1016/j.epsr.2022.108259.

[7] Q. Sun, X. Zhong, L. Zhong, F. Wang, J. Liu, S. Chen, and T. Yang, "Investigation on induced voltage of photovoltaic system on complex terrain," *Electr. Power Syst. Res.*, vol. 201, Dec. 2021, Art. no. 107549, doi: 10.1016/j.epsr.2021.107549.

[8] M. Nazari, R. Moini, S. Fortin, F. P. Dawalibi, and F. Rachidi, "Impact of frequency-dependent soil models on grounding system performance for direct and indirect lightning strikes," *IEEE Trans. Electromagn. Compat.*, vol. 63, no. 1, pp. 134–144, Feb. 2021, doi: 10.1109/TEMC.2020.2986646.

[9] F. Tossani, F. Napolitano, A. Borghetti, C. A. Nucci, A. Piantini, Y.-S. Kim, and S.-K. Choi, "Influence of the presence of grounded wires on the lightning performance of a medium-voltage line," *Electric Power Syst. Res.*, vol. 196, Jul. 2021, Art. no. 107206, doi: 10.1016/j.epsr.2021.107206.

[10] M. E. Ahmadi, M. Niasati, and M. R. Barzegar-Bafrooei, "Enhancing the lightning performance of overhead transmission lines with optimal EGLA and downstream shield wire placement in mountainous areas: A complete study," *IET Sci., Meas. Technol.*, vol. 14, no. 5, pp. 564–575, Jul. 2020, doi: 10.1049/iet-smt.2019.0074.

[11] M. Khodsuz, "Lightning evaluation of overhead transmission line protected by EGLA," *Iran. J. Electr. Electron. Eng.*, vol. 18, no. 2, p. 2370, 2022, doi: 10.22068/IJEEE.18.2.2370.

[12] K. K. Weng, W. Y. Wan, R. K. Rajkumar, and R. K. Rajkumar, "Power quality analysis for PV grid connected system using PSCAD/EMTDC," *Int. J. Renew. Energy Res.*, vol. 5, no. 1, pp. 121–132, Jan. 2015, doi: 10.20508/ijrer.v5i1.1847.g6477.

[13] A. Said, M. A. Abd-Allah, M. Mohsen, and A. I. omar, "Alleviation of the transients induced in large photovoltaic power plants by direct lightning stroke," *Ain Shams Eng. J.*, vol. 2022, Jul. 2022, Art. no. 101880, doi: 10.1016/j.asej.2022.101880.
[14] F. Giraudet. (Sep. 2017). *Line Surge Arresters: Applications, Designs, Trends, Monitoring and Recommendations*. [Online]. Available: https://www.researchgate.net/profile/Florent-Giraudet/publication/319679171_line_surge_arresters_applications_designs_trends_monitoring_and_recommendations/links/59b93b27aca27241618d2153/line-surge-arresters-applications-designs-trends-monitoring-and-reco
[15] B. Robben, "Reducing clearances by integration of externally gapped line arresters on HV transmission lines," siemens-AG INMR, Tucson, AZ, USA, Tech. Rep. 10, 2019.
[16] B. G. Halasz, B. Nemeth, and G. Gocsei, "Behavior of spark gaps with different gap distances," in *Proc. IEEE Electr. Insul. Conf. (EIC)*, Jun. 2017, pp. 266–269, doi: 10.1109/EIC.2017.8004628.
[17] L. I. C. Jimenez and M. Rock, "Measurements of surface breakdown voltage of a creeping discharge spark air gap using POM as insulation material," in *Proc. 35th Int. Conf. Lightning Protection (ICLP) XVI Int. Symp. Lightning Protection (SIPDA)*, Sep. 2021, pp. 01–05, doi: 10.1109/ICLPandSIPDA54065.2021.9627358.
[18] Y. Zhang, B. Li, Y. Du, Y. Ding, J. Cao, and J. Lv, "Effective grounding of the photovoltaic power plant protected by lightning rods," *IEEE Trans. Electromagn. Compat.*, vol. 63, no. 4, pp. 1128–1136, Aug. 2021, doi: 10.1109/TEMC.2021.3050179.
[19] X. Vallvé, M. Anzizu, and M. Ribas. (Nov. 2017). *Earthing and Lightning Overvoltage Protection for Pv Plants*. [Online]. Available: https://www.lb.undp.org/DREG
[20] Y. Hashimoto, H. Fukui, T. Yano, M. Tsukazaki, and M. Sakakiwara, "Development of current limiting arcing horn (MOV type arrester with external gap) for 22 kV power distribution line," in *Proc. 7th Asia–Pacific Int. Conf. Lightning*, Nov. 2011, pp. 36–39, doi: 10.1109/APL.2011.6111069.
[21] A. Motilal, G. Hosein, C. Ramai, S. Bahadoorsingh, and C. Sharma, "Power transformer and surge arrester modeling for fast front overvoltages using EMTP-RV," in *Proc. IEEE/PES Transmiss. Distrib. Conf. Exposit. (T&D)*, Oct. 2020, pp. 1–5, doi: 10.1109/TD39804.2020.9299989.

AHMED I. OMAR received the B.Sc. degree in electrical power and machines engineering from The Higher Institute of Engineering at El-Shorouk City, El-Shorouk Academy, Egypt, in 2011, and the M.Sc. and Ph.D. degrees in electrical power and machines from the Faculty of Engineering, Cairo University, Egypt, in 2014 and 2019, respectively. From September 2011 to September 2019, he was a Teaching Assistant at The Higher Institute of Engineering at El-Shorouk City. He currently works as an Assistant Professor at The Higher Institute of Engineering at El-Shorouk City. He is the author or coauthor of many refereed journal and conference papers. His research interests include FACTS in power systems, power quality, renewable energy, smart grid, energy efficiency, optimization, green energy, and economics.

MOUSTAFA MOHSEN was born in Asyut, Egypt, in 1996. He received the B.Sc. degree (Hons.) in electrical power and machines engineering from Assiut University, in 2019. He currently works as a Teaching Assistant with the Department of Electric Power and Machines, The Higher Institute of Engineering at El-Shorouk City, El-Shorouk Academy. His research interests include transient analysis of power systems and renewable energy studies using PSCAD/EMTDC software packages.

MOUSA A. ABD-ALLAH was born in Cairo, Egypt, in 1961. He received the B.Sc. degree (Hons.) in electrical engineering and the M.Sc. degree in high voltage engineering from Zagazig University, Benha Branch, Cairo, in 1984 and 1988, respectively, and the Ph.D. degree in high voltage engineering from Cairo University, in 1992. He is currently a Professor with the Department of Electrical Engineering, Faculty of Engineering at Shoubra, Benha University. His research interests include electromagnetic field assessment and mitigation, gas discharge in gas-insulated systems, transient phenomenon on power networks, and modern protection techniques of electrical power equipment.

ZAKARIA M. SALEM ELBARBARY was born in Kafr El-Sheikh, Egypt, in 1971. He received the B.Sc., M.Sc., and Ph.D. degrees in electrical engineering from Menoufia University, Egypt, in 1994, 2002, and 2007, respectively. In 2009, he joined Kafrelsheikh University as an Assistant Professor and Promoted to Full Professor in Power Electronics in june 2022. In 2016, he was a Research Visitor at Ghent University, Ghent, Belgium, for two months. His research interests include control of electrical machines, senseless control, applications of power electronics, real-time control using digital signals processing, and renewable energy applications.

ABDELRAHMAN SAID was born in Cairo, Egypt, in 1987. He received the B.Sc. degree (Hons.) in electrical power and machines and the M.Sc. and Ph.D. degrees in high voltage engineering from the Department of Electrical Power and Machines, Faculty of Engineering at Shoubra, Benha University, Cairo, in 2009, 2013, and 2016, respectively. He is currently working as an Associate Professor with the Department of Electrical Engineering, Faculty of Engineering at Shoubra, Benha University. His research interests include transient phenomenon in power networks, artificial intelligent in power systems, and renewable energy.